Institute of Physics Publishing Journal of Physics: Conference Series **5** (2005) 37–45
doi:10.1088/1742-6596/5/1/003 International Workshop on Particle Multiplicity in Relativistic Heavy Ion Collisions

Charged particle distributions and transverse dynamics in Au+Au and d+Au collisions at $\sqrt{s_{NN}}$=200 GeV from STAR

Jörn Putschke for the STAR collaboration[1]

Max-Planck-Institut für Physik (Werner-Heisenberg-Institut), Föhringer Ring 6, 80805 München, Germany

E-mail: putschke@mppmu.mpg.de

Abstract. Results of directed and elliptic flow measurements of charged hadrons at mid-rapidity and forward rapidities from Au+Au collisions at $\sqrt{s_{NN}}$=200 GeV will be presented. The pseudorapidity dependence of anistropic flow and mean transverse momentum will be discussed in connenction with the available particle density created in a heavy-ion collision. The measurements of the centrality dependence of $dN/d\eta$ and transverse momentum spectra from mid-rapidity to forward rapidity in d+Au collisions at 200 GeV are shown to provide a sensitive tool for understanding the dynamics of multi-particle production in the high parton density regime. In particular an explanantion of the observed centrality and pseudorapidty dependence of R_{CP} (and R_{dAu}) at forward rapidities due to the initial asymmetry in particle production in d+Au collisions compared to the symmetric p+p collisions will be presented.

1. The STAR experiment

The STAR experiment [1] at the Relativistic Heavy Ion Collidier (RHIC) measures charged hadrons over a wide range in pseudorapidity η and transverse momentum p_t. The main detector is a large TPC [2] which allows particle identification via dE/dx within the acceptance of $|\eta| < 1$. Charged particle detection in the forward directions of the STAR experiment are done with the two azimutally symmetric Forward TPCs (FTPCs [3]) which extend the pseudorapidity coverage of STAR to the region of $2.5 < |\eta| < 4$. The novel design of the FTPCs using a radial drift field perpendicular to the magnetic field allows a two-track resolution of 1-2 mm (an order of magnitude better than in a standard TPC) and therefore a nearly complete event reconstruction. Other detector subsystems which were not used in the following studies include a silicon vertex tracker, an electromagnetic calorimeter and time-of-flight patches. All results presented here are obtained from Au+Au and d+Au collisions at a center of mass energy of $\sqrt{s_{NN}}$=200 GeV.

2. Au+Au measurements

In figure 1 the first measurement of directed flow[2] at RHIC energies is shown [7]. A significant directed flow signal is only visible in the forward directions, while at mid-rapidity it is consistent

[1] For the full list of authors see [7]

[2] All anisotropic flow measurements $v_n\{m\}$ are done using the cumulant method [4, 5, 6], were n denotes the n-th order anisotropic flow and m the order of the cumulant.

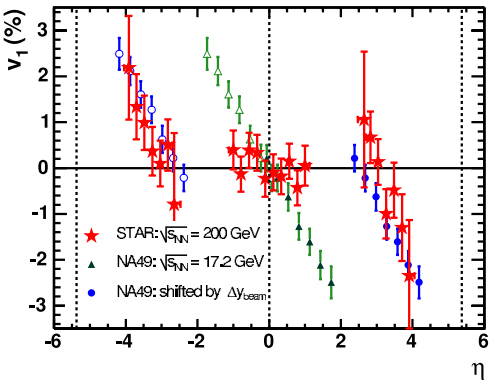

Figure 1. Directed flow v_1 (stars) for charged particles for 10% to 70% centrality plotted as a function of pseudorapidity [7]. Also shown are the results from NA49 [8] for pions from 158A GeV Pb + Pb collisions both at the measured values of η (triangles) and also shifted (circles) plus or minus by the difference in the beam rapidities of the two accelerators (Δy_{beam}). Results are from analyses involving three-particle cumulants, $v_1\{3\}$.

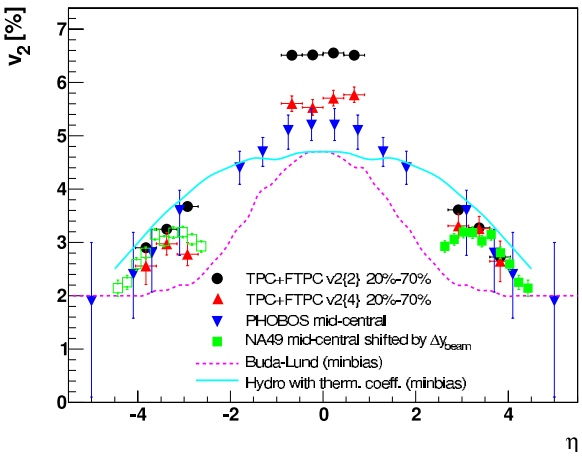

Figure 2. Elliptic flow $v_2\{2\}$ (circles) and $v_2\{4\}$ (upward triangles) as a function of η for 20% to 70% centrality. Downward triangles are mid central PHOBOS v_2 measurements [12]. Also overlayed are v_2 measurements from NA49 [8] shifted by Δy_{beam}. The full line represents predictions of Hydrodynamics including an additional thermalization-coefficient [13]. The dashed lines are calculations from the Buda-Lund-Model [14]. Model predictions are for minimum-bias Au+Au collisions.

with zero. Comparisons to v_1 measurements at lower beam energies from NA49 [8] show a greatly different behaviour of $v_1(\eta)$. But if one plots the NA49 $v_1(\eta)$ results in the projectile frame relative to their respective beam rapidities (Δy_{beam}), they are in good agreement with the directed flow measurements from STAR. This result is an indication that the limiting-fragmentation hypothesis is also applicable to directed flow measurements. The success of the limiting-fragmentation hypothesis for the particle density in Au+Au collisions was shown in detail by the PHOBOS collaboration [9]. Measurements from the STAR-FTPCs in the pseudorapidity region of $3 < |\eta| < 3.5$ confirm this conclusion [10]. The measurement of v_1 was used to determine the sign of the elliptic flow v_2 to be positive, which is equivalent to the statement that the elliptic flow is *in-plane* [11].

The measurements of elliptic flow $v_2(\eta)$ for charged hadrons at forward rapidities and in the central region are shown in figure 2 and confirm the published results by the PHOBOS collaboration at high η [15, 12]. Comparing the results of v_2 obtained from the method of two-particle cumulants $v_2\{2\}$ to that from four-particle cumulants $v_2\{4\}$ – which should be insensitive to non-flow contributions [16] – suggests that the non-flow contributions at forward rapidities are small compared to mid-rapidity. Also v_2 measurements from NA49 shifted by Δy_{beam} are overlayed in figure 2. One sees that the shifted elliptic flow values from NA49 agree with the measurements from STAR at higher rapidities $|\eta| > 2.5$. This limiting-fragmentation behaviour of v_2, also reported by the PHOBOS collaboration [17], could be due to comparable particle density and $\langle p_t \rangle$ (see figure 3 and [18]) for $|\eta| > 2.5$ at RHIC energies and mid-rapidity at SPS. This supports the idea that the fall-off of v_2 at forward rapidities is caused by incomplete thermalization and that the degree of thermalization is mainly determined by the the produced energy density in a heavy-ion collision [13].

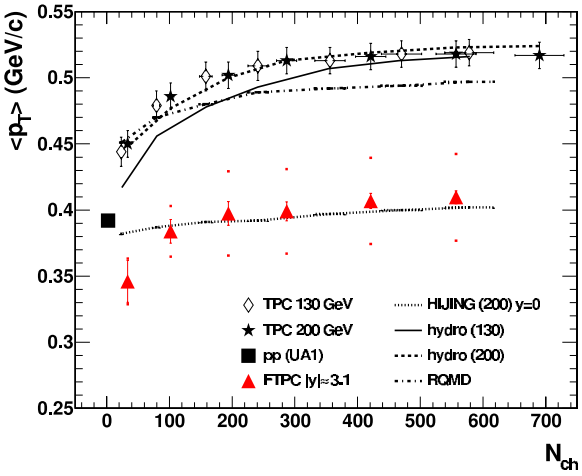

Figure 3. $\langle p_t \rangle$ at $y_\pi \approx 3.1$ measured in the FTPCs (triangles) as function of N_{ch} measured in the TPC. The stars are $\langle p_t \rangle$ measurements at 200 GeV at mid-rapidity from the TPC and the open symbols at 130 GeV. Also overlayed are predictions from HIJING, RQMD and Hydrodynamics (all for $y = 0$). The TPC measurements and the model calculations are taken from [19].

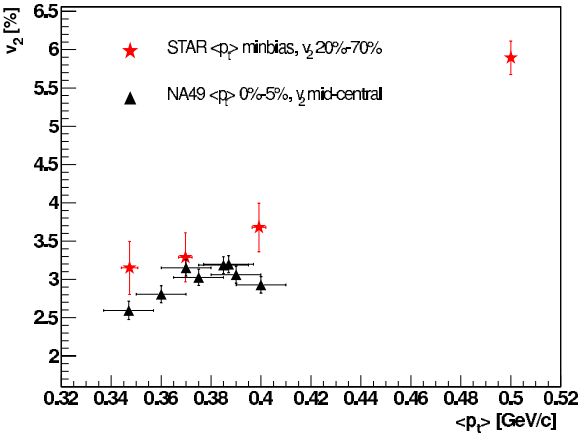

Figure 4. $v_2\{2\}$ as function of $\langle p_t \rangle$ for STAR at $\sqrt{s_{NN}}$=200 GeV (stars) and NA49 measurements at $\sqrt{s_{NN}}$=17.4 GeV [8, 18] correlated via the produced particle density $dN/d\eta$.

In figure 3 the mean transverse momentum $\langle p_t \rangle$ measured at mid-rapidity and forward rapidities is shown as a function of N_{ch} measured in the TPC. The $\langle p_t \rangle$ measurements at mid-rapidity and forward rapidities show the same characteristics, $\langle p_t \rangle$ is increasing with centrality and reaches a plateau value at high multiplicity. This behaviour can be reproduced at mid-rapidity by hydrodynamical calculations [19].

Correlating v_2 and $\langle p_t \rangle$ via the produced particle density $dN/d\eta$ (see figure 4) one is led to conclude that the transverse dynamics at $|\eta| > 3$ at RHIC is comparable to that at SPS. Therefore it seems that elliptic flow and the mean transverse momentum is mainly determined by the produced particle density, supporting the hydrodynamical picture that the system at higher rapidities and lower energies did not reach complete thermalization.

Taking also the directed flow and particle density measurements into account, the data suggest that the initial conditions of the system created in a heavy-ion collision at high rapidities at RHIC are simular to those at lower SPS energies in the central rapidity region.

3. d+Au measurements

3.1. Particle density

In figure 5 the pseudorapidity distribution $dN_{ch}/d\eta$ of charged hadrons in the TPC and FTPC acceptance for 0-20%, 20-40%, 40-100% central and minimum bias d+Au events is shown. For comparison, measurements of the pseudorapidity distribution from PHOBOS [20, 21] and BRAHMS [22] are also plotted. The measured $dN_{ch}/d\eta$ distributions for minimum bias d+Au events are in very good agreement for all three experiments. Whereas, with increasing centrality, a significant difference in the particle density at negative pseudorapidity values $\eta <$ -3 on the Au-side of a d+Au collision between STAR and PHOBOS is visible. On the other hand, the measurements in the central pseudorapidity region are in good agreement. The

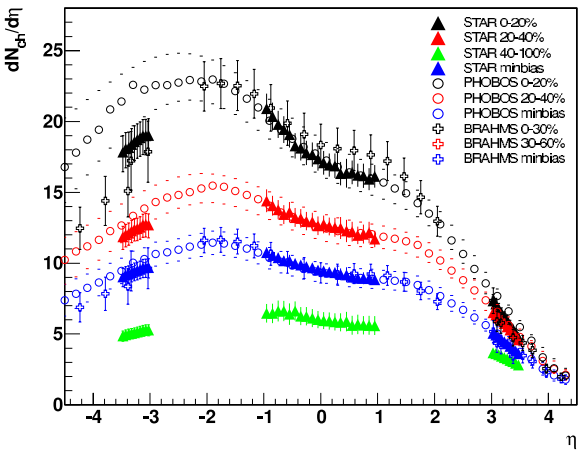

Figure 5. Pseudorapidity distribution of charged hadrons in the TPC and FTPC acceptance for 0-20%, 20-40%, 40-100% central and minimum bias d+Au events (triangles). The error bars include statistical and systematic error. Also overlayed are measurements from BRAHMS (crosses) [22] and PHOBOS (circles) [20, 21].

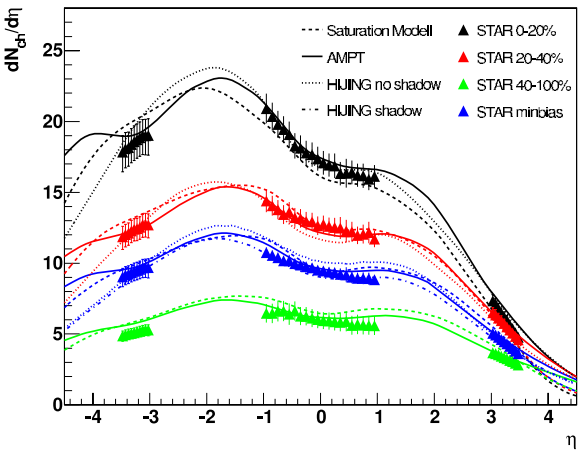

Figure 6. Pseudorapidity distribution of charged hadrons in the TPC and FTPC acceptance for 0-20%, 20-40%, 40-100% central and minimum bias d+Au events (triangles) (see also figure 5). In addition predictions from HIJING [23], AMPT [24] and the Saturation Model [25] are also plotted.

BRAHMS measurements show the opposite behaviour compared to the STAR results. A possible explanation could be the different methods used for centrality selection. To avoid autocorrelations in the measured multiplicty due to fluctuations, the centrality selection for the STAR-TPC was done via the N_{ch} multiplicity in the FTPC and vice versa. It was found that this method, due to a pseudorapidity gap of 2 units between the detectors, is insensitive to autocorrelations and simulations show that similar event classes are selected. If one uses instead the FTPC N_{ch} multiplicity on the Au-side to define centrality a significant bias to higher particle densities is visible for the $dN_{ch}/d\eta$ distribution for $\eta <$ -3 [10]. This observation explains the higher particle density measured by PHOBOS for the Au-side of a d+Au collisions, because their centrality was determined via the multiplicity in the pseudorapidity region of -4 $< \eta <$ -3.5. On the other hand, the enhancement in the particle density at mid-rapidity from BRAHMS could be due to the fact that they use the multiplicty in the central region $|\eta| < 2.2$ to define centrality. But it should be noted that within the systematic errors the results of all three experiments are consistent.

In figure 6 the pseudorapidity distribution $dN_{ch}/d\eta$ of charged hadrons in the TPC and FTPC acceptance for various centrality classes and minimum bias d+Au events (see also figure 5) is shown. Calculations based on the ideas of gluon saturation in the Color Glass Condensate [25] as well as results of HIJING [23] and AMPT [24] are also shown. All model calculations are in good overall agreement with the measured $dN_{ch}/d\eta$ distributions for different centrality classes. Especially they are able to reproduce the increasing asymmetry of charged particle densities with increasing centrality.

3.2. Nuclear modification

As shown in section 3.1 all models are basically able to reproduce the measured particle density as function of pseudorapidity and centrality. Therefore with the measurement of this quantity one can not distinguish between different model assumptions.

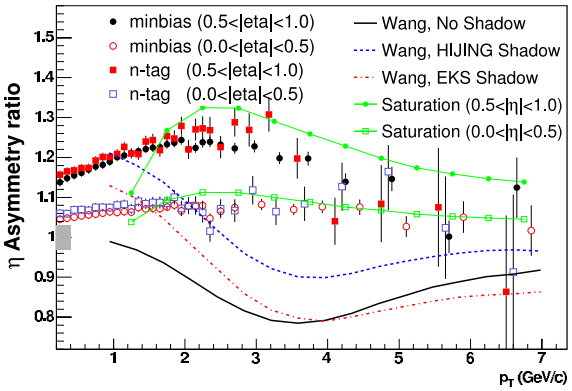

Figure 7. Ratio of charged hadron spectra in the backward to forward rapidity region for minimum bias and ZDC-d neutron tagged events. pQCD calculations at ($y = \pm 1$) with different shadowing and calculations from gluon saturation are also shown [26].

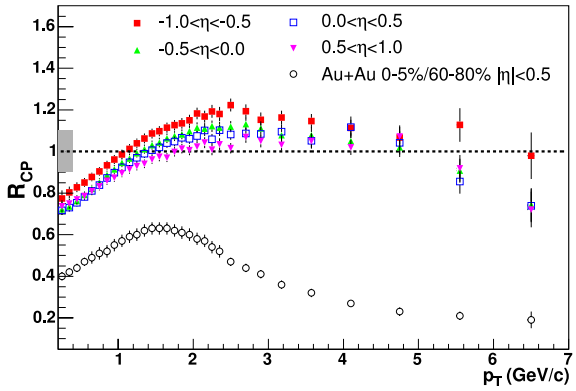

Figure 8. R_{CP} (0-20%/40-100%) for d+Au events measured in the TPC for various pseudorapidity regions and in Au+Au collisions at mid-rapidity [26].

For better discrimination one can study the asymmetry by taking the ratios of backward (Au-side) to forward (d-side) transverse momentum spectra around mid-rapidity. In figure 7 the asymmetry as function of p_t for minimum bias and ZDC-d neutron tagged events is plotted [26]. ZDC-d neutron tagged events are a separate centrality class, which requires that a single neutron hits the Zero Degree Calorimeter in the deuteron beam direction. When interpreting particle production at mid-rapidity in d+Au collisions, contributions from the d-side partons which have experienced multiple scatterings, and contributions from the Au-side partons which could be modified by nuclear effects have to be taken into account. Comparing the measurements with theoretical calculations (see figure 7) one finds that models assuming incoherent multiple scattering of partons in the inital state can not reproduce the measured asymmetry, while new calculations based on gluon saturation are in qualitative agreement (a detailed discussion can be found in [26]).

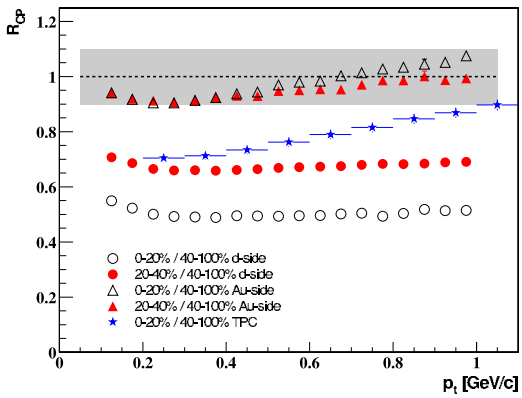

Figure 9. R_{CP} at $\eta \approx$ -3.1 (Au-side; triangles) and at $\eta \approx 3.1$ (d-side; circles) for 0-20%, 20-40% central d+Au events. The grey band represents the estimate of the systematic error. Also measurements of R_{CP} at mid-rapidity for 0-20% central d+Au events are plotted [26].

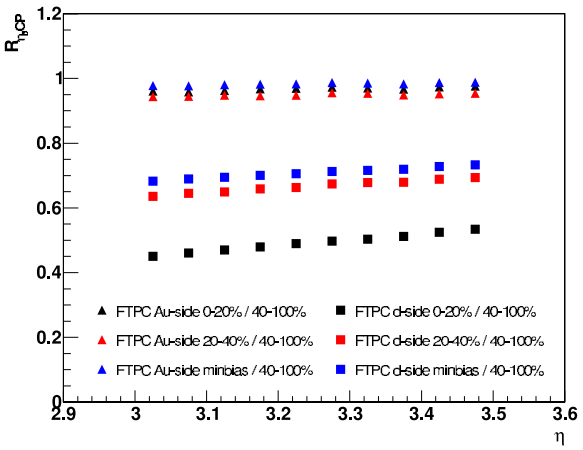

Figure 10. $R_{\eta,CP}$ on the Au-side (triangles) and d-side (boxes) for 0-20%, 20-40%, 40-100% central and minimum bias d+Au events.

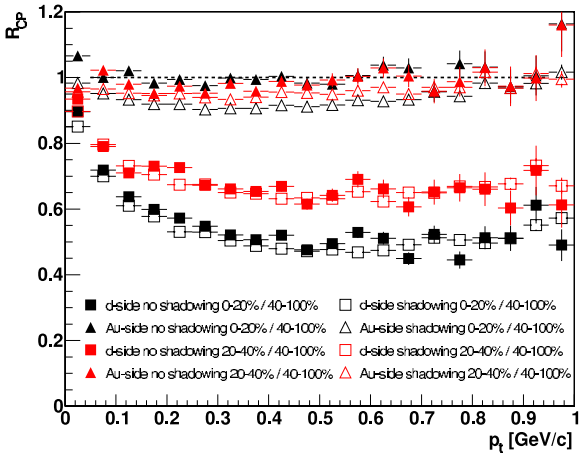

Figure 11. R_{CP} at $\eta \approx$ -3.1 (Au-side; triangles) and at $\eta \approx 3.1$ (d-side; boxes) for 0-20%, 20-40% central d+Au HIJING events. Open symbols denote HIJING simulations including shadowing, closed symbols without shadowing.

Another variable of interest is the ratio of central to peripheral inclusive d+Au spectra

$$R_{CP}(p_t) = \frac{(d^2N/dp_t d\eta/\langle N_{bin}\rangle)|_{central}}{(d^2N/dp_t d\eta/\langle N_{bin}\rangle)|_{periph}}, \qquad (1)$$

where $d^2N/dp_t d\eta$ is the differential yield per event and $\langle N_{bin}\rangle$ the mean number of binary collisions for the corresponding centrality class, calculated using a Monte Carlo Glauber model [27]. Figure 8 shows R_{CP} for various pseudorapidity windows around mid-rapidity [26]. At low p_t the value of R_{CP} is highest for the most backward pseudorapidity region and decreases if one goes to forward rapidities. Looking at higher rapidities $|\eta| \approx 3.1$ (see figure 9) the same trend of R_{CP} is visible for $p_t < 1$ GeV/c, which indicates that the Cronin effect is more pronounced on the Au-side of a d+Au collision. Another interesting feature in figure 9 is the strong centrality dependence of R_{CP} on the d-side of the collisions, also reported by the BRAHMS collaboration [28]. However on the Au-side of a d+Au collisions there is no significant centrality dependence. The suppression of R_{CP} (and R_{dAu}) at higher rapidities on the d-side is in qualitative agreement with predictions of the Saturation Model [25]. On the other hand QCD models can also describe the behaviour of R_{CP} at higher rapidities [29, 30].

In the following paragraph I would like to discuss the centrality dependence of R_{CP} at high rapidities $|\eta| \approx 3.1$ in connection with the observed increasing asymmetry of the produced particle density in d+Au collisions at low transverse momentum $p_t < 1$ GeV/c. In figure 10 an analogous quantity to R_{CP} (see equation (1)) namely $R_{\eta,CP}$ is plotted as a function of η for different centrality classes. Comparing $R_{\eta,CP}$ to R_{CP} the same characteristic centrality dependence especially on the d-side of a d+Au collision is visible. Also the absolute values of R_{CP} are reflected in $R_{\eta,CP}$. In figure 11 R_{CP} from HIJING simulations for different centralities with and without shadowing is shown. Comparing figure 11 with figure 9 one can see that HIJING reproduces the behaviour of R_{CP} at $|\eta| \approx 3.1$. In addition figure 11 shows that the influence of shadowing for $p_t < 1$ GeV/c seems to be small. Since one observes that the p_t spectrum on the d-side is more or less independent of centrality (see section 3.3 below) and

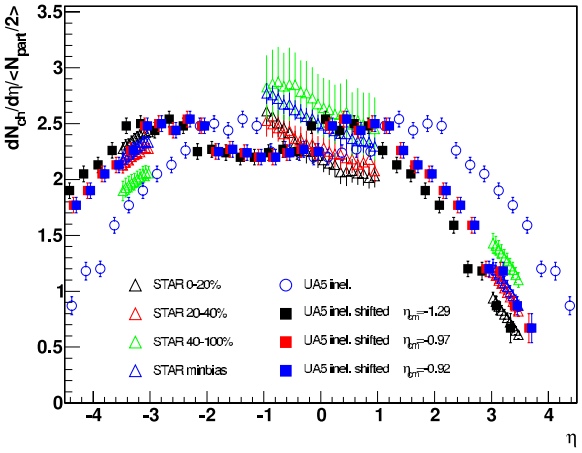

Figure 12. Pseudorapidity distribution of charged hadrons in the TPC and FTPC acceptance for 0-20%, 20-40%, 40-100% central and minimum bias d+Au events scaled with N_{part} (triangles). Also overlayed are p+p measuremnts [31] shifted by η_{cm} (boxes) (for further details see text).

comparable with p+p collisions, the suppression of the nuclear modification factor on the d-side could be due to the initial asymmetry in particle production in d+Au collisions with respect to the symmetric p+p collisions (see figure 12). To take the initial asymmetry in d+Au collisions into account a new variable η_{cm} is introduced, which is defined as the weighted mean of the $dN_{ch}/d\eta$ distribution for each centrality class. η_{cm} was extracted from the published PHOBOS results [21] (η_{cm} = -1,29, -0,97 and -0,92 for 0-20%, 20-40% and minimum bias d+Au events) and should represent the shift of the center of mass in the asymmetric d+Au collisions with respect to the nucleon-nucleon center of mass system. The inelastic p+p collisions [31] in this new reference system – obtained by shifting with η_{cm} – are shown in figure 12. One observes that the d+Au $dN_{ch}/d\eta$ distributions normalized with $\langle N_{part}/2\rangle$ at high rapidities are consistent with the shifted p+p values. Also the centrality dependence can be qualitatively explained. Therefore η_{cm} seems to be the appropriate variable to describe the asymmetry in particle production in d+Au collisions.

In summary it should be noted that the suppression and enhancement of R_{CP} (and R_{dAu}) at high rapidities and $p_t < 1$ GeV/c can also be explained through a shift of the center of mass in the asymmetric d+Au collisions with respect to the symmetric p+p collisions.

3.3. Centrality dependence of $\langle p_t \rangle$

Figure 13 shows the $\langle p_t \rangle$ extracted from fitting the transverse momentum spectra with a power law function as function of N_{part}. In contrast to the "naive" picture in which the partons from the d-nucleus experience multiple collisions while traversing the Au-nucleus and therefore get an enhancement of $\langle p_t \rangle$ on the d-side of the collision [32], a significant increase of $\langle p_t \rangle$ with increasing centrality on the Au-side is visible, whereas on the d-side basically no centrality dependence of $\langle p_t \rangle$ is present. This observation is consistent with the measurements of R_{CP} shown in section 3.2.

4. Conclusions

The measurements of directed flow and $dN/d\eta$ in Au+Au collisions at $\sqrt{s_{NN}}$=200 GeV are consistent with the limiting-fragmentation hypothesis. Moreover $\langle p_t \rangle$ and elliptic flow v_2 at higher rapidites at RHIC energies are in agreement with measurements at lower SPS energies at mid-rapidity. This suggests that $\langle p_t \rangle$ and v_2 are mainly determined by the produced particle density in a heavy-ion collision and supports the idea of Heinz and Kolb [13] that the system at higher rapidities did not reach complete thermalization due to lower available energy density. In summary it appears that the initial conditions of the system created in a heavy-ion collision

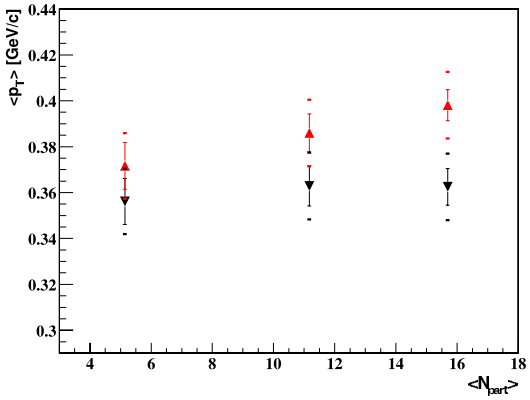

Figure 13. $\langle p_t \rangle$ at $|\eta| \approx 3.1$ as function of N_{part}. The upward triangels are $\langle p_t \rangle$ measurements on the Au-side of a d+Au collision at $\eta \approx$ -3.1 and the downward triangles are $\langle p_t \rangle$ measurements on the d-side of a d+Au collision at $\eta \approx 3.1$.

at high rapidities at RHIC are simular to those at lower SPS energies in the central rapidity region.

In d+Au collisions at $\sqrt{s_{NN}}$=200 GeV the $dN/d\eta$ distributions as function of centrality were presented. It was shown that the centrality selection used in STAR is insensitive to autocorrelations and therefore avoids additional bias in the pseudorapidity spectra. Within the errors $dN/d\eta$ can not discriminate between different model calculations. A significant increase of $\langle p_t \rangle$ as function of centrality was observed on the Au-side, whereas on the d-side no centrality dependence is visible. This result and the suppression of R_{CP} on the d-side and the enhancement on the Au-side compared to mid-rapidity can not be described consistently by current model calculations [32]. An alternative explanation of the pseudorapidity and centrality dependence of R_{CP} (and R_{dAu}) was also presented, in which the suppression and enhancement of R_{CP} (and R_{dAu}) at high rapidities and $p_t < 1$ GeV/c was explained by the inital asymmetry in particle production in d+Au collisions compared to the symmetric p+p collisions.

Acknowledgments

We thank the RHIC Operations Group and RCF at BNL, and the NERSC Center at LBNL for their support. This work was supported in part by the HENP Divisions of the Office of Science of the U.S. DOE; the U.S. NSF; the BMBF of Germany; IN2P3, RA, RPL, and EMN of France; EPSRC of the United Kingdom; FAPESP of Brazil; the Russian Ministry of Science and Technology; the Ministry of Education and the NNSFC of China; Grant Agency of the Czech Republic, FOM and UU of the Netherlands, DAE, DST, and CSIR of the Government of India; Swiss NSF; and the Polish State Committee for Scientific Research.

References

[1] Ackermann K H *et al* 2003 *Nucl. Inst. Meth.* A **499** 624
[2] Anderson M *et al* 2003 *Nucl. Inst. Meth.* A **499** 659
[3] Ackermann K H *et al* 2003 *Nucl. Inst. Meth.* A **499** 713
[4] Borghini N, Dinh P M and Ollitrault J 2001 *Phys. Rev.* C **63** 054906
[5] Borghini N, Dinh P M and Ollitrault J 2001 *Phys. Rev.* C **64** 054901
[6] Borghini N, Dinh P M and Ollitrault J 2002 *Phys. Rev.* C **66** 014905
[7] Adams J *et al* 2004 *Phys. Rev. Lett.* **92** 062301
[8] Alt C *et al* 2003 *Phys. Rev.* C **68** 034903
[9] Back B B *et al* 2003 *Phys. Rev. Lett.* **91** 052303
[10] Putschke J 2004 Thesis Max-Planck-Institut für Physik München To be published
[11] Oldenburg M *Preprint* nucl-ex/0403007

[12] Back B B *et al* *Preprint* nucl-ex/0403025
[13] Heinz U and Kolb P *Preprint* nucl-th/0403044
[14] Csanad M, Csorgo T and Lorstad B *Preprint* nucl-th/0402036
[15] Back B B *et al* 2002 *Phys. Rev. Lett.* **89** 222301
[16] Adler C *et al* 2002 *Phys. Rev.* C **66** 034904
[17] Back B B *et al* *Preprint* nucl-ex/0406021
[18] Appelshauser H *et al* 1999 *Phys. Rev. Lett.* **82** 2471
[19] Adams J *et al* 2004 in preparation
[20] Back B B *et al* *Preprint* nucl-ex/0311009
[21] Nouicer R *et al* *Preprint* nucl-ex/0403033
[22] Arsene I *et al* *Preprint* nucl-ex/0401025
[23] Wang X and Gyulassy M 1991 *Phys. Rev.* D **44** 3501
[24] Lin Z and Ko C M 2003 *Phys. Rev.* C **68** 054904
[25] Kharzeev D, Levin E and Nardi M 2004 *Nucl. Phys.* A **730** 448
[26] Adams J *et al* *Preprint* nucl-ex/0408016
[27] Adams J *et al* 2003 *Phys. Rev. Lett.* **91** 072304
[28] Arsene I *et al* *Preprint* nucl-ex/0403005
[29] Vitev I 2003 *Phys. Lett.* B **562** 36
[30] Wang X 2003 *Phys. Lett.* B **565** 116
[31] Alner G J *et al* 1986 *Z. Phys.* C **33** 1
[32] Accardi A *Preprint* nucl-th/0405046